IRON ABUNDANCES ON THE LUNAR SURFACE AS MEASURED BY THE LUNAR PROSPECTOR GAMMA-RAY SPECTROMETER. D. J. Lawrence[1], W. C. Feldman[1], D. T. Blewett[4], R. C. Elphic[1], P. G. Lucey[4], S. Maurice[2], T. H. Prettyman[1], and A. B. Binder[3], [1]Los Alamos National Laboratory, Group NIS-1, MS D466, Los Alamos, NM 87544 (djlawrence@lanl.gov); [2]Observatoire Midi-Pyrénées, Toulouse, France; [3]Lunar Research Institute, Tucson, Arizona; [4]University of Hawaii, Honolulu, Hawaii.

Introduction: Measurements of global iron abundances on the Moon's surface are important for addressing many lunar science problems such as understanding theories of lunar formation, the Moon's bulk composition, and the formation, distribution and variety of lunar mare basalts. While the iron abundances at the Apollo landing sites have been well characterized using returned sample measurements [1], quantitative and accurate measurements of global iron abundances have been more difficult to obtain. However, since the time of the Apollo missions, a number of regional and global iron abundance measurements have been made using a variety of remote sensing techniques such as gamma-ray spectroscopy [2], Clementine Spectral Reflectance (CSR) [3], and neutron spectroscopy [4]. Here we present the first quantitative estimates of global iron abundances from the Lunar Prospector Gamma-Ray Spectrometer (LP-GRS) data.

Measured γ-ray count rate: For this study, we are deriving Fe abundances using the measured counting rate of 7.6 MeV γ-rays produced by neutron capture reactions [5]. For a given location on the lunar surface (λ, φ,=lat, lon), the counting rate, R, of 7.6 MeV Fe gamma-rays (measured using an energy window technique [6]) follows the relation [7]:

$$R(\lambda,\varphi) = n(\lambda,\varphi)N_{norm}(\lambda,\varphi)C\ ,$$

where n is the iron atom abundance, N_{norm} is a normalized thermal neutron number density, and C is a calculated constant factor which depends on various nuclear physics and viewing geometry parameters. The neutron number density is closely related to the measured thermal neutron flux and therefore varies by over a factor three across the Moon [8]. Because of this large variation, it is crucial that the measured γ-ray count rate (Figure 1) be corrected for the neutron number density. Fortunately, the neutron number density can be quantitatively measured using data from the Lunar Prospector Neutron Spectrometer (LP-NS) [7]. Figure 2 shows the results when the 7.6 MeV count rate is corrected for neutron number density (the absolute Fe abundance scale was derived by regression with CSR data, see next section). The effect of the neutron number density correction is immediately seen by comparing Figures 1 and 2. For example, in Mare Tranquillitatis and western Procellarum, the count rate intensity is clearly suppressed in Figure 1 compared to the corrected map in Figure 2. This count rate suppression is due to the presence of high abundances of titanium, gadolinium, and samarium which are strong thermal neutron absorbers [8]. In contrast, the relatively high count rates seen in the highlands of Figure 1 are suppressed in the map corrected for neutron number density (Figure 2).

Comparison with CSR data: Figure 3 shows a map of CSR derived abundances [3] smoothed to the LP-GRS footprint. Figure 4 shows a scatter plot comparing iron abundances derived from LP-GRS and CSR measurements divided into three regions: 1) eastern mare and highlands (black circles); 2) western mare and highlands (red circles); and 3) southern latitudes (blue circles). Inspection shows that the correlation between the two datasets for all combined regions is quite good. However, the three selected regions each show distinct trends. First, the correlation of the two datasets in the eastern mare is almost perfectly linear (R=0.97). Since this is the region which includes most of the ground truth measurements which are the foundation of the CSR algorithm [9], we would expect this region to have the best agreement. In fact, we have set our LP-GRS absolute Fe scale using the measured correlation in the eastern mare and highlands. In contrast, the GRS-CSR trend in the western mare regions shows a clear non-linearity at high Fe abundances. Derivation of the CSR Fe algorithm did not include data with Fe contents as high as the western mare, or as low as the lunar farside. We can now see that the relationship between the derived CSR Fe-sensitive parameter and Fe is distinctly non-linear. Including this nonlinearity in the CSR calibration will remove most of the discrepancies between the data sets observed. However, the nonlinearity cannot account for the differences observed in the South Pole-Aitken Basin. Specifically, the Fe abundances in the southern latitudes which are dominated by South Pole Aitken Basin show a completely different trend such that at even moderate abundances, the CSR measurements are systematically higher than the LP-GRS measurements. These results indicate that the chemical associations which characterize the dominant mineralogy in SPA may be fundamentally different from the chemical associations which characterize the mineralogies of the sample collection [10].

References: [1] Haskin, L and Warren (1991) *The Lunar Sourcebook*, 357 – 474; [2] Davis, P. A. (1980) *JGR*, *85*, 3209 – 3224 [3] Lucey et al. (2000) *JGR*, 105, #E8, 20297 – 20305; [4] Feldman et al., (2000) *JGR*, 105 #E8, 20347 – 20363; [5] Reedy, R. C. (1978) *Proc. Lunar Plan. Sci Conf. 9th*, 2961 – 2984; [6] Lawrence et al., (2000) *JGR*, 105 #E8, 20307 – 20331; [7] Lawrence et al. (2001) *JGR*, in preparation; [8] Elphic et al. (2000) *JGR*, 105, #E8, 20333 – 20345; [9] Blewett et al. (1997) *JGR*, 102, #E7, 16319 – 16325; [10] Lucey et al., (2001) *Lunar Planet. Sci. 32nd*, Abstract #1761.

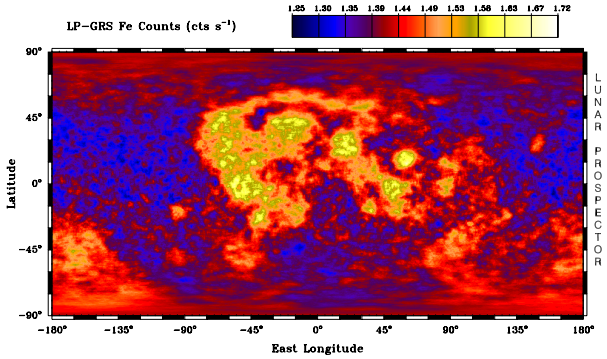

Figure 1: Count rate map of 7.6 MeV γ-ray line.

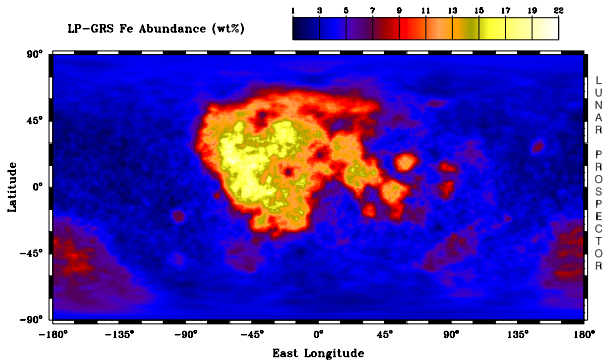

Figure 2: LP-GRS derived Fe abundances.

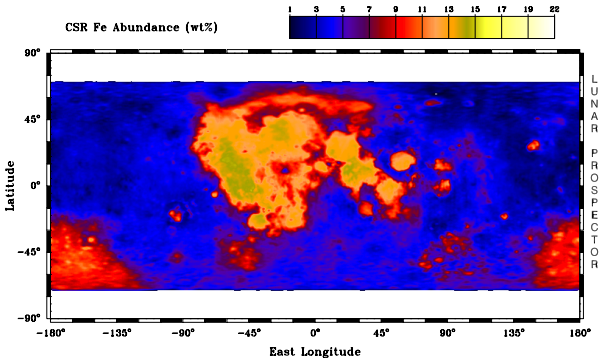

Figure 3: CSR Fe abundances smoothed to the LP-GRS footprint.

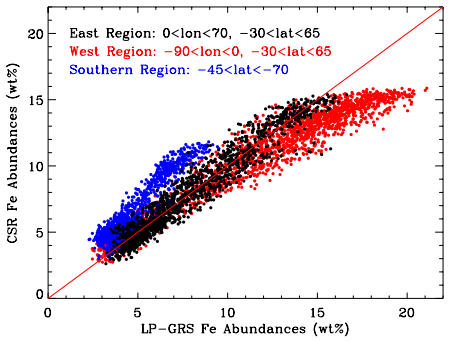

Figure 4: Comparison of LP-GRS and CSR derived Fe abundances.